Prdm16 is required for the maintenance of neural stem cells in the postnatal forebrain and their differentiation into ependymal cells

Issei S. Shimada,[1,2] Melih Acar,[1,2,3] Rebecca J. Burgess,[1,2] Zhiyu Zhao,[1,2] and Sean J. Morrison[1,2,4]

[1]Children's Research Institute, [2]Department of Pediatrics, University of Texas Southwestern Medical Center, Dallas, Texas 75390, USA; [3]Bahcesehir University, School of Medicine, Istanbul 34734, Turkey; [4]Howard Hughes Medical Institute, University of Texas Southwestern Medical Center, Dallas, Texas 75390, USA

We and others showed previously that PR domain-containing 16 (Prdm16) is a transcriptional regulator required for stem cell function in multiple fetal and neonatal tissues, including the nervous system. However, *Prdm16* germline knockout mice died neonatally, preventing us from testing whether Prdm16 is also required for adult stem cell function. Here we demonstrate that Prdm16 is required for neural stem cell maintenance and neurogenesis in the adult lateral ventricle subventricular zone and dentate gyrus. We also discovered that Prdm16 is required for the formation of ciliated ependymal cells in the lateral ventricle. Conditional *Prdm16* deletion during fetal development using Nestin-Cre prevented the formation of ependymal cells, disrupting cerebrospinal fluid flow and causing hydrocephalus. Postnatal *Prdm16* deletion using *Nestin*-CreER^{T2} did not cause hydrocephalus or prevent the formation of ciliated ependymal cells but caused defects in their differentiation. Prdm16 was required in neural stem/progenitor cells for the expression of Foxj1, a transcription factor that promotes ependymal cell differentiation. These studies show that Prdm16 is required for adult neural stem cell maintenance and neurogenesis as well as the formation of ependymal cells.

[*Keywords*: Prdm16; ependymal cell; hydrocephalus; neural stem cell]

Supplemental material is available for this article.

Received October 8, 2016; revised version accepted June 12, 2017.

Neural stem cells give rise to the cerebral cortex during fetal development (Lui et al. 2011) and persist throughout adult life in the forebrain (Alvarez-Buylla et al. 2008). In the adult forebrain, neural stem cells reside in the lateral wall of the lateral ventricle, where they give rise to transient amplifying progenitors, which differentiate into neuroblasts that migrate to the olfactory bulb and form interneurons (Doetsch et al. 1999; Alvarez-Buylla et al. 2008), as well as in the subgranular layer of the dentate gyrus, where they form granule neurons (Aimone et al. 2014). In the lateral ventricle subventricular zone (SVZ), neural stem cells are highly quiescent Glast$^+$GFAP$^+$Sox2$^+$ cells (Doetsch et al. 1999; Ferri et al. 2004; Codega et al. 2014; Mich et al. 2014). These cells give rise to mitotically active, but multipotent, neurosphere-initiating cells, which express lower levels of GFAP and Glast and are relatively short-lived in the brain (Codega et al. 2014; Mich et al. 2014). These multipotent progenitors in turn give rise to neuroblasts and differentiated neurons (Lim and Alvarez-Buylla 2014). The SVZ also contains astrocytes, endothelial cells, and ependymal cells, each of which regulates neural stem cell function and neurogenesis (Lim et al. 2000; Mirzadeh et al. 2008; Porlan et al. 2014).

Ependymal cells are multiciliated cells that line the walls of the ventricles in the central nervous system (CNS) and promote the directional flow of cerebrospinal fluid (CSF) (Sawamoto et al. 2006; Mirzadeh et al. 2010b; Faubel et al. 2016). CSF contains cytokines that are critical for the maintenance and proliferation of neural stem cells, and CSF flow regulates neuroblast migration (Sawamoto et al. 2006). Depletion of ciliated ependymal cells disrupts the flow of CSF, resulting in the accumulation of CSF and the swelling of ventricles, a condition known as hydrocephalus (Jacquet et al. 2009; Del Bigio 2010; Tissir et al. 2010; Ohata et al. 2014). Hydrocephalus affects 0.1% of infants and is associated with disruption of CNS architecture and intellectual developmental delays (Fliegauf et al. 2007; Tully and Dobyns 2014). Hydrocephalus can be caused by blockage of CSF flow, overproduction of CSF by the choroid plexus, reduced absorption of CSF at

Corresponding author: sean.morrison@utsouthwestern.edu
Article published online ahead of print. Article and publication date are online at http://www.genesdev.org/cgi/doi/10.1101/gad.291773.116.

arachnoid granulations, or defects in ependymal cell function, but many cases of congenital hydrocephalus remain unexplained (Del Bigio 2010; Tully and Dobyns 2014; Kahle et al. 2016).

Ependymal cells arise from neural stem cells during fetal development and fully differentiate by the second week of postnatal life (Tramontin et al. 2003; Spassky et al. 2005). Some of the mechanisms that regulate the differentiation of ependymal cells have been identified. Two proteins that are homologous to geminin—Mcidas and GemC1—promote the expression of the Foxj1 and c-Myb transcription factors, all of which are necessary for ependymal cell differentiation (Malaterre et al. 2008; Jacquet et al. 2009; Stubbs et al. 2012; Tan et al. 2013; Kyrousi et al. 2015). The transcription factors Trp73 (Yang et al. 2000; Gonzalez-Cano et al. 2016), Yap (Park et al. 2016), and Gli3 (Wang et al. 2014) and the kinase Ulk4 (Liu and Guan 2016) are also required for ependymal cell differentiation. There are also many genes that, when mutated, impair cilia function and can contribute to the development of hydrocephalus (Fliegauf et al. 2007; Tissir et al. 2010; Ohata et al. 2014).

The PR domain-containing (Prdm) family contains 16 members that function as transcriptional regulators and methyltransferases in diverse cell types (Hohenauer and Moore 2012). Prdm16 was found originally in leukemias, where truncation mutants are oncogenic (Mochizuki et al. 2000; Nishikata et al. 2003; Shing et al. 2007). Prdm16 promotes stem cell maintenance in the fetal hematopoietic and nervous systems (Chuikov et al. 2010; Aguilo et al. 2011; Luchsinger et al. 2016) as well as brown fat cell differentiation from skeletal muscle precursors (Seale et al. 2008; Cohen et al. 2014). Microdeletion of a chromosome 1 locus that includes *Prdm16* in humans causes 1p36 deletion syndrome, affecting one in 5000 newborns. 1p36 deletion syndrome is associated with congenital heart disease, hydrocephalus, seizures, and developmental delay. Prdm16 is necessary for normal heart development in humans (Battaglia et al. 2008) and zebrafish (Arndt et al. 2013). However, it is unknown whether *Prdm16* deletion contributes to hydrocephalus.

We and others found that germline deletion of *Prdm16* impairs the maintenance of neural stem cells and hematopoietic stem cells during fetal development (Chuikov et al. 2010; Aguilo et al. 2011). However, *Prdm16* germline knockout mice die at birth; therefore, it is not known whether Prdm16 is required for the maintenance or differentiation of neural stem cells postnatally. In this study, we conditionally deleted *Prdm16* in fetal and adult neural stem cells. We found that Prdm16 was required for adult neural stem cell maintenance and neurogenesis as well as the differentiation of neural stem/progenitor cells into ependymal cells.

Results

Fetal deletion of Prdm16 *leads to hydrocephalus and thinning of the SVZ*

We assessed the *Prdm16* expression pattern in the adult SVZ by localizing β-galactosidase (β-gal) expression in 2- to 3-mo-old $Prdm16^{LacZ/+}$ ($Prdm16^{Gt(OST67423)Lex}$) mice (Bjork et al. 2010). β-Gal was broadly expressed in the SVZ of these mice (Fig. 1A–D), including nearly all $GFAP^+$ cells (which include quiescent neural stem cells and astrocytes) (Fig. 1A–D; Doetsch et al. 1999; Codega et al. 2014; Mich et al. 2014), DCX^+ neuroblasts (Fig. 1B–D; Gleeson et al. 1999), and $S100B^+$ ependymal cells (Spassky et al. 2005) lining the lateral wall of the lateral ventricle (the SVZ ventricular surface) (Fig. 1C,D). Thus, Prdm16 is expressed broadly in the adult SVZ, including within neural stem cells, neural progenitors, and ependymal cells.

To test whether *Prdm16* is required for postnatal neural stem cell function, we conditionally deleted it using *Nestin*-Cre (Tronche et al. 1999; Cohen et al. 2014). Most *Nestin-Cre; $Prdm16^{fl/fl}$* mice survived into adulthood. We confirmed that *Prdm16* was efficiently deleted from the SVZ of 2- to 3-mo-old adult *Nestin-Cre; $Prdm16^{fl/fl}$* mice by quantitative RT–PCR (qRT–PCR) on unfractionated SVZ cells (Fig. 1E) as well as neurospheres cultured from the SVZ (Supplemental Fig. S1A). PCR on genomic DNA from individual neurospheres from *Nestin-Cre; $Prdm16^{fl/fl}$* mice showed that 100% exhibited deletion of both *Prdm16* alleles (Supplemental Fig. S1A).

Nestin-Cre; $Prdm16^{fl/fl}$ mice had normal body mass (Fig. 1F) and brain mass (Fig. 1G), but brain morphology differed from littermate controls. Littermate controls were a combination of $Prdm16^{fl/fl}$, $Prdm16^{fl/+}$, and $Prdm16^{+/+}$ mice. We did not observe any phenotypic differences among mice with these genotypes. Adult *Nestin-Cre; $Prdm16^{fl/fl}$* mice had hydrocephalus marked by enlarged lateral ventricles (Fig. 1H,I; Fliegauf et al. 2007; Tully and Dobyns 2014). The SVZ was significantly thinner in adult *Nestin-Cre; $Prdm16^{fl/fl}$* mice than in littermate controls (Fig. 1J,K), and the olfactory bulb was significantly smaller (Fig. 1L,M). However, the corpus callosum and cortex were similar in thickness in *Nestin-Cre; $Prdm16^{fl/fl}$* mice and littermate controls (Fig. 1N; Supplemental Fig. S1B). Thus, *Prdm16* deficiency in neural stem/progenitor cells led to hydrocephalus, thinning of the adult SVZ, and reduced olfactory bulb size.

Prdm16 is required for adult neural stem cell function and neurogenesis

To determine whether Prdm16 regulates adult neural stem cells, we analyzed neural stem cell function and neurogenesis in the adult SVZ. Quiescent neural stem cells (type B cells), which can be identified as $GFAP^+$ $Sox2^+S100B^-$ cells (Doetsch et al. 1999), were profoundly depleted in the SVZ of 2- to 3-mo-old *Nestin-Cre; $Prdm16^{fl/fl}$* mice as compared with littermate controls (Fig. 2A). $GLAST^{mid}EGFR^{high}PlexinB2^{high}CD24^{-/low}O4/PSA\text{-}NCAM^{-/low}Ter119/CD45^-$ (GEPCOT) cells, which are highly enriched for neurosphere-initiating cells (Mich et al. 2014), were also significantly depleted in the SVZ of *Nestin-Cre; $Prdm16^{fl/fl}$* mice as compared with littermate control mice (Fig. 2B; Supplemental Fig. S1C). Dissociated SVZ cells from *Nestin-Cre; $Prdm16^{fl/fl}$* mice formed significantly fewer neurospheres than control SVZ cells (Fig. 2C,D), and the *Prdm16*-deficient neurospheres were

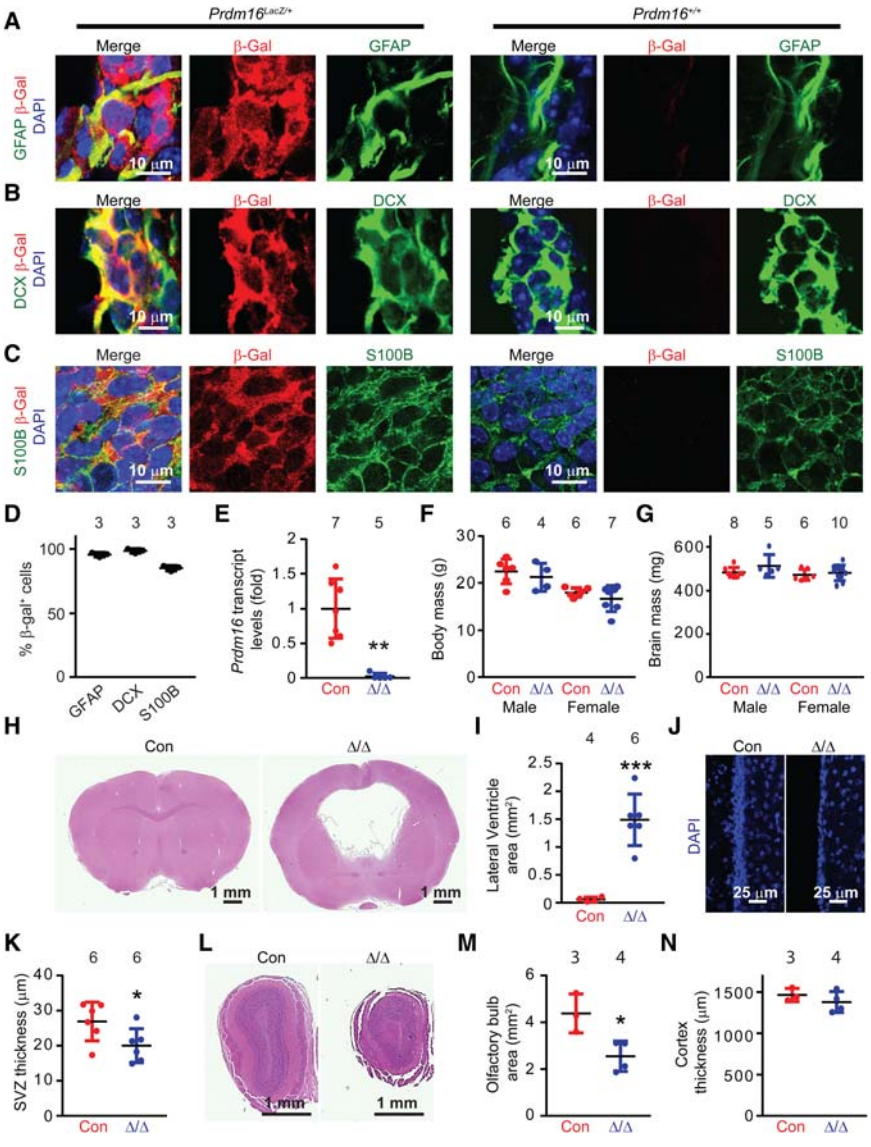

Figure 1. Prdm16 acts in neural stem/progenitor cells to regulate forebrain development. (*A–C*) In the SVZ of 2- to 3-mo-old *Prdm16*$^{LacZ/+}$ mice, β-gal colocalized with GFAP (*A*), DCX (*B*), and S100B (*C*). Coronal sections (GFAP and DCX) or en face images of the ventricular surface (S100B) are shown. (*D*) Most GFAP$^+$ cells, DCX$^+$ neuroblasts, and S100B$^+$ ependymal cells were β-gal$^+$ (two independent experiments). (*E–N*) All mice were 2- to 3-mo-old *Nestin-Cre; Prdm16*$^{fl/fl}$ (Δ/Δ) or littermate controls (Con; *Prdm16*$^{fl/fl}$), and all data represent mean ± SD. (*E*) Quantitative RT–PCR (qRT–PCR) analysis of *Prdm16* transcript levels in SVZ cells (two independent experiments). (*F,G*) Body (*F*) and brain (*G*) mass (six independent experiments). (*H*) Hematoxylin and eosin-stained coronal sections showing enlarged lateral ventricles in *Nestin-Cre; Prdm16*$^{fl/fl}$ mice. (*I*) Lateral ventricle area. Measurements were performed in four to five coronal sections per mouse, each 300 μm apart, beginning at the rostral end of the lateral ventricle (three independent experiments). (*J,K*) Representative images (*J*) and thickness measurements (*K*) of DAPI staining in coronal SVZ sections (three independent experiments). (*L,M*) Hematoxylin and eosin-stained coronal sections of the olfactory bulb. The cross-sectional area was measured in four to five coronal sections per mouse, taken 300 μm apart, beginning at the caudal olfactory bulb when no cortex was evident in the sections (three independent experiments). (*N*) Cortical thickness (from the dorsolateral lateral ventricle to the cortical surface, excluding the white matter) was measured in four to five coronal sections per mouse, taken 300 μm apart, beginning at the rostral end of the lateral ventricle (three independent experiments). The statistical significance of differences between genotypes was assessed by two-way ANOVAs with Sidak's multiple comparisons tests (*F,G*), Mann-Whitney test (*E*), or Student's *t*-tests (*I,K,M,N*). (*) $P < 0.05$; (***) $P < 0.001$. The numbers of replicates in each treatment are shown at the *top* of each graph.

significantly smaller than control neurospheres (Fig. 2C, E). In contrast to control neurospheres, almost no *Prdm16*-deficient neurospheres underwent multilineage differentiation into TuJ1$^+$ neurons, GFAP$^+$ astrocytes, and O4$^+$ oligodendrocytes (Fig. 2F). *Prdm16*-deficient neurospheres also failed to form multipotent daughter neurospheres upon dissociation and subcloning into secondary cultures, in contrast to control neurospheres (Fig. 2G). These data suggest that Prdm16 is required for the formation or maintenance of neural stem cells and neurosphere-initiating cells in the adult SVZ.

Prdm16 was also required for normal neurogenesis in the SVZ. Although we did not detect any difference in the frequency of cells undergoing cell death in the SVZ of *Nestin-Cre; Prdm16*$^{fl/fl}$ as compared with control mice (Fig. 2H), we did observe significantly fewer dividing cells in the *Nestin-Cre; Prdm16*$^{fl/fl}$ SVZ based on Ki67 staining (Fig. 2I,J) and incorporation of a 2-h pulse of BrdU (Fig. 2K). Consistent with this, neurogenesis was profoundly reduced in the SVZ of *Nestin-Cre; Prdm16*$^{fl/fl}$ mice as compared with control mice, with significantly fewer DCX$^+$ cells (Fig. 2L,M) and PSA-NCAM$^+$CD24$^+$ neuroblasts (Fig. 2N).

Prdm16 was also required for neurogenesis in the dentate gyrus. The morphology of the dentate gyrus was distorted in *Nestin-Cre; Prdm16*$^{fl/fl}$ mice as compared with littermate controls (Fig. 2O). *Nestin-Cre; Prdm16*$^{fl/fl}$ mice had significantly reduced frequencies of Ki67$^+$ cells (Fig. 2P), cells that incorporated a 2-h pulse of BrdU (Fig. 2Q), DCX$^+$ cells (Fig. 2R), and NeuroD1$^+$ cells (Fig. 2S) in the subgranular layer as compared with littermate controls.

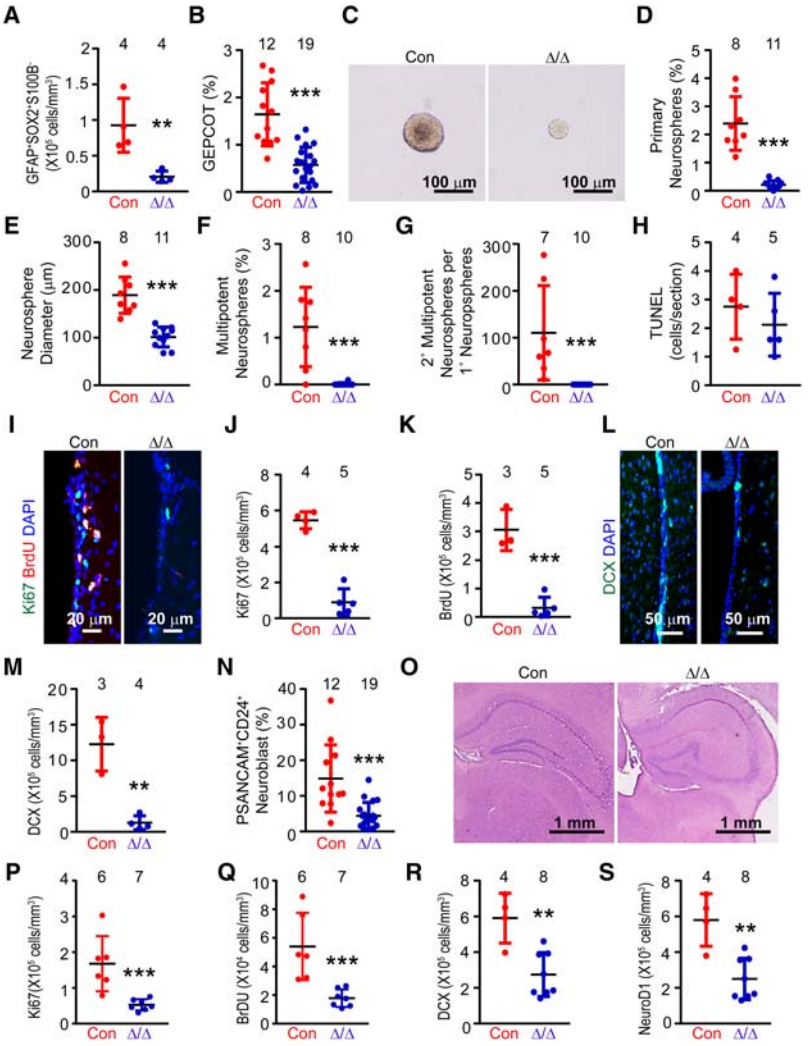

Figure 2. Prdm16 regulates the self-renewal and multipotency of adult neural stem/progenitor cells. All mice were 2- to 3-mo-old *Nestin-Cre; Prdm16$^{fl/fl}$* (Δ/Δ) or littermate controls (Con), and all data represent mean ± SD. (*A*) The number of GFAP$^+$Sox2$^+$S100B$^-$ type B neural stem cells in the SVZ (three independent experiments). (*B*) The frequency of GEPCOT neurosphere-initiating cells as a percentage of all live SVZ cells (nine independent experiments). (*C–G*) Representative neurospheres (*C*), the percentage of SVZ cells that formed primary neurospheres (>50 μm in diameter) when cultured at clonal density (*D*), primary neurosphere diameter (*E*), the percentage of SVZ cells that formed neurospheres that underwent multilineage differentiation (neurons, astrocytes, and oligodendrocytes) (*F*), and the number of secondary multipotent neurospheres derived from a single primary neurosphere upon subcloning (*G*). *D–G* reflect data from six independent experiments. (*H–M*) The number of TUNEL$^+$ apoptotic cells per SVZ section (*H*), the number of Ki67$^+$ proliferating cells in the SVZ (*I,J*), the number of SVZ cells that incorporated a 2-h pulse of BrDU (*K*), and the number of DCX$^+$ neuroblasts in the SVZ (*L,M*). *H–M* reflect data from three independent experiments. (*N*) The frequency of PSA-NCAM$^+$CD24$^+$ neuroblasts as a percentage of all live SVZ cells (six independent experiments). (*O–S*) Data reflect analyses of the subgranular zone (SGZ) of the dentate gyrus in four independent experiments. (*O*) Hematoxylin and eosin-stained coronal sections through the dentate gyrus. (*P*) The number of Ki67$^+$ proliferating cells per section in the SGZ of the dentate gyrus. (*Q*) The number of cells that incorporated a 2-h pulse of BrdU in the SGZ. (*R,S*) The number of DCX$^+$ cells (*R*) and NeuroD1$^+$ neuroblasts (*S*) in the SGZ of the dentate gyrus. The statistical significance of differences between genotypes was assessed using Mann-Whitney tests (*F,G*), Welch's test (*B*), or Student's *t*-tests (*A,D,E,H,J,K,M,N,P–S*). (**) $P < 0.01$; (***) $P < 0.001$. The numbers of replicates in each treatment are shown at the *top* of each graph.

Prdm16 is required for adult neural stem cell function

In the experiments above, it was not clear to what extent the defects in brain morphology, stem cell function, and neurogenesis in *Prdm16*-deficient mice reflected a developmental requirement for Prdm16 versus ongoing functions in the adult forebrain. To address this, we conditionally deleted *Prdm16* from young adult neural stem/progenitor cells using *Nestin-CreER^{T2}* (Balordi and Fishell 2007). Although Nestin is expressed at a lower level in quiescent neural stem cells as compared with neurosphere-initiating cells (Codega et al. 2014), *Nestin-CreER^{T2}* recombines in both cell populations (Mich et al. 2014). *Nestin-CreER^{T2}; Prdm16$^{fl/fl}$* mice and littermate controls were administered tamoxifen for 1 mo starting at 2 mo of age and then analyzed 2 wk, 3 mo, or 6 mo after finishing tamoxifen treatment (at 3.5, 6, or 9 mo of age). *Nestin-CreER^{T2}; Prdm16$^{fl/fl}$* mice and littermate controls rarely died during these experiments and had similar body masses (Supplemental Fig. S2A).

One month after tamoxifen treatment, we confirmed that *Prdm16* was efficiently deleted from the SVZ of *Nestin-CreER^{T2}; Prdm16$^{fl/fl}$* mice by qRT–PCR using unfractionated SVZ cells (Fig. 3A). PCR analysis of genomic DNA from individual neurospheres cultured from the SVZ of *Nestin-CreER^{T2}; Prdm16$^{fl/fl}$* mice showed that 96% exhibited deletion of both *Prdm16* alleles (24 of 25 neurospheres from three mice) (Supplemental Fig. S2B). We did not detect any signs of hydrocephalus in *Nestin-CreER^{T2}; Prdm16$^{fl/fl}$* mice at 3 mo after tamoxifen treatment (Fig. 3B,C). This demonstrates that the hydrocephalus observed in *Nestin-Cre; Prdm16$^{fl/fl}$* mice reflected a loss of Prdm16 function during fetal and/or early postnatal development.

At 2 wks after tamoxifen treatment, the frequencies of GFAP$^+$Sox2$^+$S100B$^-$ quiescent neural stem cells (Doetsch et al. 1999) and GEPCOT neurosphere-initiating cells (Mich et al. 2014) in the SVZ did not significantly differ between *Nestin-CreER^{T2}; Prdm16$^{fl/fl}$* mice and littermate controls (Fig. 3D,E). However, the frequencies of

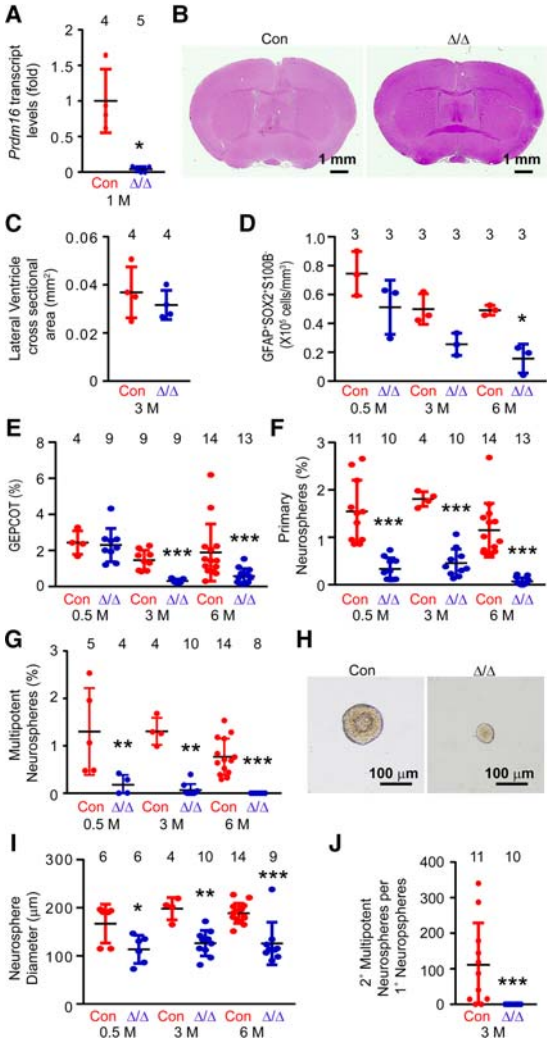

Figure 3. Prdm16 acts intrinsically within adult neural stem/progenitor cells to regulate self-renewal potential and multipotency. *Nestin-CreER^{T2}*; *Prdm16$^{fl/fl}$* (Δ/Δ) and littermate controls (Con) were treated with tamoxifen for 1 mo beginning at 2 mo of age and then analyzed 0.5, 3, or 6 mo after the completion of tamoxifen treatment. All data represent mean ± SD. (*A*) *Prdm16* transcript levels in the SVZ by qRT–PCR 1 mo after tamoxifen treatment. (*B*) Representative images of hematoxylin and eosin-stained coronal sections. (*C*) Lateral ventricle cross-sectional area (four to five sections per mouse, cut 300 μm apart). (*D*) The number of GFAP$^+$Sox2$^+$S100B$^-$ type B neural stem cells per cubic millimeter in the SVZ. (*E*) The frequency of GEPCOT neurosphere-initiating cells as a percentage of all live SVZ cells. (*F*) The percentage of SVZ cells that formed primary neurospheres (>50 μm in diameter) at clonal density in culture. (*G*) The percentage of SVZ cells that formed neurospheres that underwent multilineage differentiation. (*H*,*I*) Representative images (*H*) and diameters (*I*) of neurospheres. (*J*) The number of secondary multipotent neurospheres produced per single primary neurosphere upon subcloning (three to six primary neurospheres subcloned per mouse from five independent experiments). The statistical significance of differences between genotypes was assessed using the Mann-Whitney test (*J*), Welch's test (*A*), Student's *t*-tests (*C*), or two-way ANOVAs with Sidak's multiple comparisons tests (*D*—*G*,*I*). (*) $P < 0.05$; (**) $P < 0.01$; (***) $P < 0.001$. The numbers of replicates in each treatment are shown at the *top* of each graph.

GFAP$^+$Sox2$^+$S100B$^-$ quiescent neural stem cells at 6 mo after tamoxifen treatment and GEPCOT neurosphere-initiating cells at 3 and 6 mo after tamoxifen treatment were significantly lower in the SVZs of *Nestin-CreER^{T2}*; *Prdm16$^{fl/fl}$* mice (Fig. 3D,E). Dissociated SVZ cells from *Nestin-CreER^{T2}*; *Prdm16$^{fl/fl}$* mice formed significantly fewer neurospheres—and fewer neurospheres that underwent multilineage differentiation—as compared with control SVZ cells at 2 wk, 3 mo, and 6 mo after tamoxifen treatment (Fig. 3F,G; Supplemental Fig. S2C–E). *Prdm16*-deficient neurospheres were significantly smaller than control neurospheres at each time point analyzed (Fig. 3H,I) and failed to self-renew upon subcloning to secondary cultures (Fig. 3J). Therefore, there is an ongoing requirement for Prdm16 in adult neural stem cells and neurosphere-initiating cells in the SVZ in vivo.

There was also an ongoing requirement for Prdm16 for progenitor proliferation in the adult SVZ. We did not detect any difference in the frequency of cells undergoing cell death in the SVZ of *Nestin-CreER^{T2}*; *Prdm16$^{fl/fl}$* as compared with control mice (Supplemental Fig. S2F). The frequency of dividing cells in the SVZ of *Nestin-CreER^{T2}*; *Prdm16$^{fl/fl}$* mice did not significantly differ from littermate controls at 2 wk after tamoxifen treatment based on the frequency of Ki67$^+$ cells or the incorporation of BrdU (Fig. 4A–C); however, the frequencies of Ki67$^+$ cells and BrdU$^+$ cells were significantly reduced in the SVZs of *Nestin-CreER^{T2}*; *Prdm16$^{fl/fl}$* mice as compared with littermate controls at 3 and 6 mo after tamoxifen treatment (Fig. 4B,C).

Nestin-CreER^{T2}; *Prdm16$^{fl/fl}$* mice also exhibited reduced neurogenesis. The frequency of DCX$^+$ neuroblasts did not significantly differ between the SVZs of *Nestin-CreER^{T2}*; *Prdm16$^{fl/fl}$* and littermate control mice at 2 wk after tamoxifen treatment but was significantly reduced in *Nestin-CreER^{T2}*; *Prdm16$^{fl/fl}$* mice at 3 and 6 mo after tamoxifen treatment (Fig. 4D,E). The frequency of PSA-NCAM$^+$CD24$^+$ neuroblasts was also significantly reduced in the SVZs of *Nestin-CreER^{T2}*; *Prdm16$^{fl/fl}$* mice as compared with control mice at 3 and 6 mo after tamoxifen treatment (Fig. 4F). The frequency of newborn BrdU$^+$ NeuN$^+$ neurons in the olfactory bulb was also significantly reduced in *Nestin-CreER^{T2}*; *Prdm16$^{fl/fl}$* mice as compared with control mice after tamoxifen treatment (Fig. 4G,H).

There was also an ongoing requirement for Prdm16 for proliferation and neurogenesis in the dentate gyrus of the adult hippocampus. The morphology of the dentate gyrus was not significantly altered in *Nestin-CreER^{T2}*; *Prdm16$^{fl/fl}$* mice as compared with littermate controls (Supplemental Fig. S2G). However, *Nestin-CreER^{T2}*; *Prdm16$^{fl/fl}$* mice had significantly fewer Ki67$^+$ cells, BrdU$^+$ cells, DCX$^+$ cells, and NeuroD1$^+$ cells in the subgranular layer as compared with littermate controls after tamoxifen treatment (Supplemental Fig. S2H–K).

To assess whether Prdm16 is required for neural stem cell function in the adult SVZ, we treated *Nestin-CreER^{T2}*; *Prdm16$^{fl/fl}$* and littermate control mice with three daily doses of temozolomide starting 2 wk after the end of tamoxifen treatment (Fig. 4I). Temozolomide depletes dividing progenitors, including GEPCOT

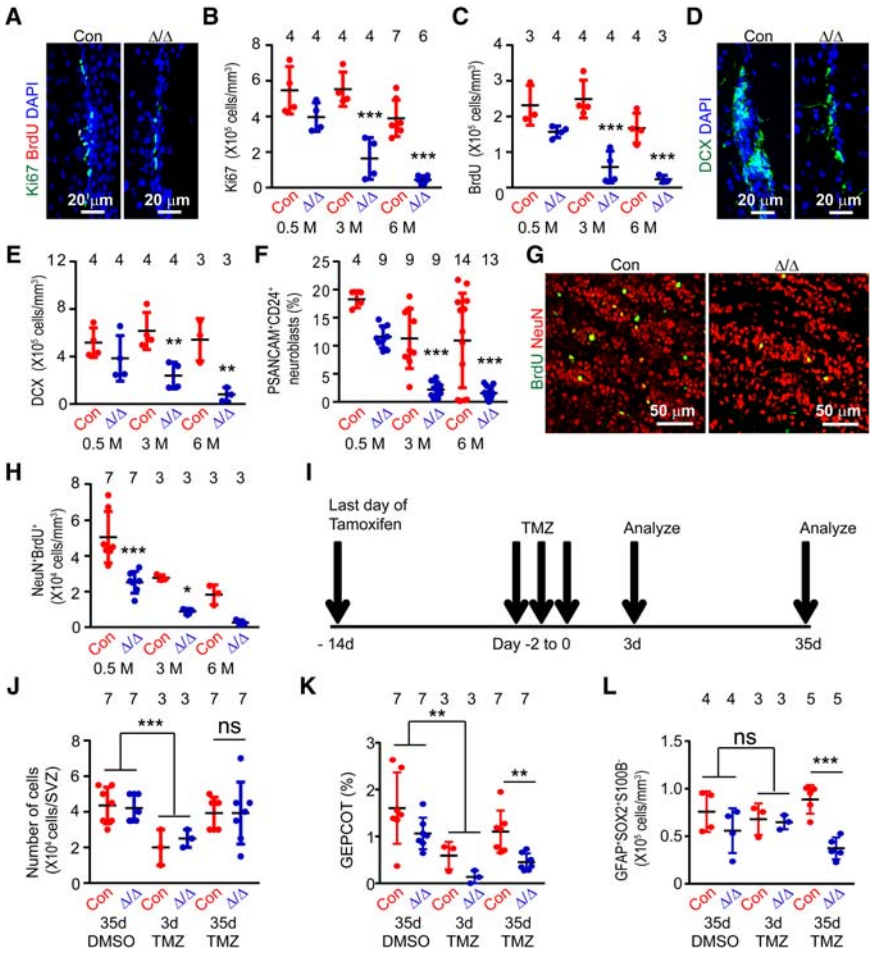

Figure 4. Prdm16 acts intrinsically within adult neural stem/progenitor cells to promote neurogenesis and SVZ regeneration. *Nestin-CreER^{T2}*; *Prdm16$^{fl/fl}$* (Δ/Δ) and littermate controls (Con) were treated with tamoxifen for 1 mo beginning at 2 mo of age and then analyzed 0.5, 3, or 6 mo after the completion of tamoxifen treatment. All data represent mean ± SD. (*A*) Ki67, BrdU, and DAPI staining in the SVZ 3 mo after tamoxifen treatment. (*B*,*C*) The number of Ki67$^+$ proliferating cells (*B*) and cells that incorporated a 2-h pulse of BrdU (*C*) per cubic millimeter of SVZ. (*D*) DCX and DAPI staining in the SVZ 3 mo after tamoxifen treatment. (*E*) DCX$^+$ neuroblasts per cubic millimeter of SVZ. (*F*) The frequency of PSA-NCAM$^+$CD24$^+$ neuroblasts in the SVZ. (*G*,*H*) Representative images (*G*) and numbers (*H*) of BrdU$^+$NeuN$^+$ newborn neurons in the olfactory bulb 3 mo after tamoxifen treatment. BrdU was administered for 1 wk beginning at the indicated times after tamoxifen treatment, and then the mice were chased (no BrdU) for 1 mo before analysis. (*I*–*L*) Two weeks after the last day of tamoxifen treatment, mice were injected with 100 mg/kg temozolomide (TMZ) per day for three consecutive days to ablate proliferating cells and then allowed to recover for 3–35 d before analysis. (*J*) The total numbers of cells per SVZ. (*K*) The number of GEPCOT neurosphere-initiating cells per SVZ. (*L*) The number of GFAP$^+$Sox2$^+$S100B$^-$ type B neural stem cells per cubic millimeter of SVZ. The statistical significance of differences between genotypes (*B*,*C*,*E*,*F*,*H*) or time points (*J*–*L*) was assessed by two-way ANOVAs with Sidak's multiple comparisons tests. (*J*–*L*) The significance of differences between genotypes at the temozolomide 35-d time point was assessed using Student's *t*-tests. (*) $P < 0.05$; (**) $P < 0.01$; (***) $P < 0.001$; (ns) not statistically significant. The numbers of replicates in each treatment are shown at the *top* of each graph.

neurosphere-initiating cells, from the SVZ (Mich et al. 2014). These cells are then regenerated from quiescent stem cells over a 30-d period (Mich et al. 2014). Relative to untreated controls, we observed a significant decline in the total number of cells and the number of GEPCOT cells per SVZ in both *Nestin-CreER^{T2}*; *Prdm16$^{fl/fl}$* and littermate control mice 3 d after temozolomide treatment (Fig. 4J,K). There was no significant difference between *Nestin-CreER^{T2}*; *Prdm16$^{fl/fl}$* and littermate control mice in the total cells per SVZ at any time point (Fig. 4J). However, *Nestin-CreER^{T2}*; *Prdm16$^{fl/fl}$* mice had significantly fewer GEPCOT cells and GFAP$^+$Sox2$^+$S100B$^-$ neural stem cells in the SVZ at 35 d after temozolomide treatment as compared with littermate controls (Fig. 4K,L). These data suggest that quiescent neural stem cells in the adult SVZ depend on Prdm16 to regenerate neurosphere-initiating cells after temozolomide treatment.

Prdm16 is required for the formation of ependymal cells

To better understand the consequences of *Prdm16* deletion in the SVZ, we examined ependymal cells in *Nestin-Cre; Prdm16$^{fl/fl}$* mice (Fig. 1H–K). The number of GFAP$^-$Sox2$^+$S100B$^+$ ependymal cells (Brazel et al. 2005; Kuo et al. 2006) was significantly reduced in *Nestin-Cre; Prdm16$^{fl/fl}$* mice as compared with littermate control mice (Fig. 5A,C). Instead of GFAP$^-$Sox2$^+$S100B$^+$ ependymal cells, the ventricular surface was lined by GFAP$^+$ Sox2$^+$S100B$^+$ cells in *Nestin-Cre; Prdm16$^{fl/fl}$* mice (Fig. 5A,B). We rarely observed such cells in control mice (Fig. 5B). The GFAP$^+$Sox2$^+$S100B$^+$ cells had a radial glial cell-like morphology with long processes that extended into the cortex (Fig. 5A). Ependymal cells in littermate controls did not have such processes (Fig. 5A). Given that *Nestin-Cre; Prdm16$^{fl/fl}$* SVZ cells were unable to form multipotent neurospheres in culture (Fig. 2F), the GFAP$^+$ Sox2$^+$S100B$^+$ cells on the ventricular surface could not have been functional radial glia. Nonetheless, these observations suggested that Prdm16 is required for the formation of normal ependymal cells and that *Prdm16* deficiency caused the ventricular surface to be lined by glia rather than ependymal cells.

Ependymal cells are multiciliated and promote directional CSF flow. We visualized ependymal cilia by

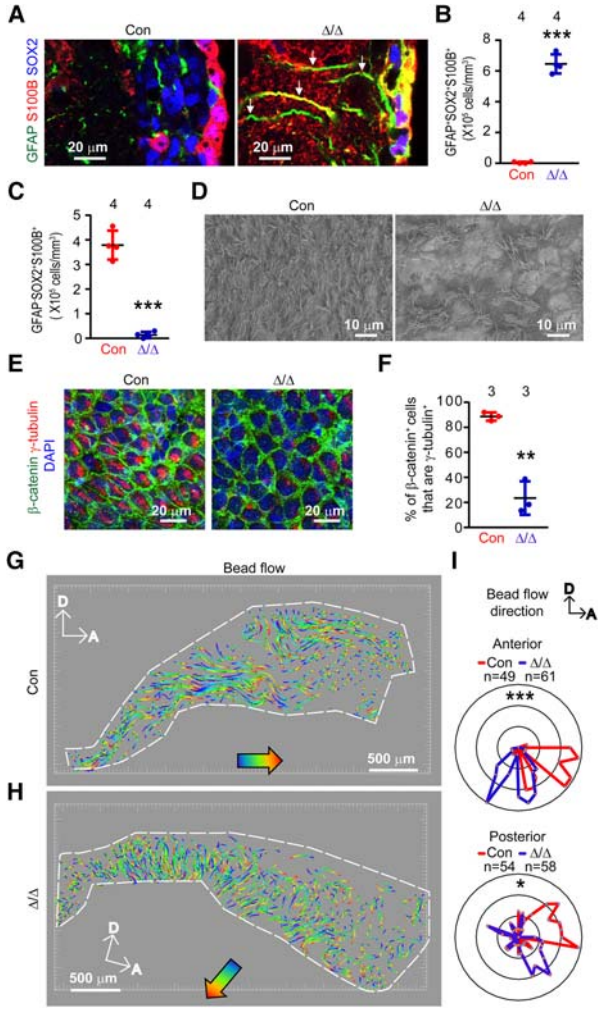

Figure 5. Prdm16 is required for the generation of ependymal cells. Two-month-old to 3-mo-old *Nestin-Cre; Prdm16*$^{fl/fl}$ (Δ/Δ) and littermate controls (Con). All data represent mean ± SD from three independent experiments. (*A,B*) GFAP$^+$S100B$^+$Sox2$^+$ cells with long processes were observed in the SVZ of *Nestin-Cre; Prdm16*$^{fl/fl}$ mice but not in littermate controls (arrows indicate radial glial-like processes). (*C*) GFAP$^-$Sox2$^+$S100B$^+$ ciliated ependymal cells were abundant on the ventricular surface of the control mouse SVZ but not the *Nestin-Cre; Prdm16*$^{fl/fl}$ mouse SVZ. (*D*) Scanning electron microscopy revealed abundant ciliated ependymal cells on the lateral wall of the lateral ventricle in control mice but not in *Nestin-Cre; Prdm16*$^{fl/fl}$ mice. (*E,F*) γ-Tubulin$^+$β-catenin$^+$ ciliated ependymal cells were abundant on the ventricular surface of the control SVZ but not the *Nestin-Cre; Prdm16*$^{fl/fl}$ SVZ. (*G–I*) Representative images of bead flow tracks on the ventricular surface of SVZ specimens in culture. Beads tended to flow anteriorly over control SVZs and posteriorly/ventrally over *Nestin-Cre; Prdm16*$^{fl/fl}$ SVZs. "D" indicates dorsal, and "A" indicates anterior. (*I*) Anterior and posterior regions of the SVZ were selected rostral or caudal to the adhesion point (three SVZs per genotype in three independent experiments). Each circle indicates 5% of the total number of microbeads. The statistical significance of differences between genotypes was assessed using the Mann-Whitney test (*I*, posterior), Welch's test (*B*), and Student's *t*-tests (*C,F,I* anterior). (*) $P < 0.05$; (**) $P < 0.01$; (***) $P < 0.001$. The numbers of replicates or beads analyzed in each treatment are shown at the *top* of each graph.

scanning electron microscopy. We observed profuse ciliated ependymal cells on the lateral wall of the lateral ventricle (the SVZ ventricular surface) in control mice but rarely in *Nestin-Cre; Prdm16*$^{fl/fl}$ mice (Fig. 5D). In agreement with this, immunofluorescence staining revealed γ-tubulin$^+$β-catenin$^+$ ciliated ependymal cells lining the lateral ventricle of control mice but rarely in *Nestin-Cre; Prdm16*$^{fl/fl}$ mice (Fig. 5E,F). Thus, Prdm16 is necessary for the formation of ciliated ependymal cells.

To examine whether *Nestin-Cre; Prdm16*$^{fl/fl}$ mice exhibit defects in cilia movement, we added fluorescently labeled microbeads to the lateral ventricle surface of freshly dissected SVZs in culture and analyzed the movement of the beads by live imaging (Mirzadeh et al. 2010a; Faubel et al. 2016). On a control en face lateral ventricle, the beads flowed anteriorly (Fig. 5G,I), consistent with the direction of CSF flow in vivo (Mirzadeh et al. 2010a; Faubel et al. 2016). In contrast, on a *Nestin-Cre; Prdm16*$^{fl/fl}$ lateral ventricle, beads flowed ventrally in the posterior half of the specimen and not in any consistent orientation in the anterior half (Fig. 5H,I). Since disruptions in CSF flow are sufficient to cause hydrocephalus, our data raise the possibility that the hydrocephalus observed in *Nestin-Cre; Prdm16*$^{fl/fl}$ mice reflects the failure of ependymal cells to differentiate or function normally.

To test whether Prdm16 is required for the maintenance of ependymal cells in adult mice, we treated *Nestin-CreER*^{T2}; *Prdm16*$^{fl/fl}$ mice with tamoxifen at 2 mo of age and then examined ependymal cell morphology and function 2 to 4 mo later. Deletion of *Prdm16* from the adult SVZ did not affect the number of GFAP$^-$ Sox2$^+$S100B$^+$ ependymal cells on the lateral ventricle surface (Supplemental Fig. S3A,B), the number of γ-tubulin$^+$β-catenin$^+$ ciliated ependymal cells (Supplemental Fig. S3C–F), or the percentage of β-catenin$^+$ cells that were γ-tubulin$^+$ (Supplemental Fig. S3E). We rarely observed GFAP$^+$SOX2$^+$S100B$^+$ cells in the SVZ of *Nestin-CreER*^{T2}; *Prdm16*$^{fl/fl}$ mice or littermate controls (Supplemental Fig. S3G). We observed no significant difference between *Nestin-CreER*^{T2}; *Prdm16*$^{fl/fl}$ mice and littermate controls in the flow of fluorescent microbeads over the ventricular surface in culture (Supplemental Fig. S3H–J). This suggests that the hydrocephalus observed in *Nestin-Cre; Prdm16*$^{fl/fl}$ mice reflects a failure of ependymal cell formation, as we did not observe either hydrocephalus or defects in ependymal cell development in *Nestin-CreER*^{T2}; *Prdm16*$^{fl/fl}$ mice.

To test whether Prdm16 is required for the postnatal differentiation of ependymal cells, we treated *Nestin-CreER*^{T2};*Prdm16*$^{fl/fl}$ mice and littermate controls with tamoxifen at postnatal day 0 (P0) and P2. We then assessed ependymal cell differentiation and the presence of hydrocephalus at 1 mo of age (Fig. 6A). *Prdm16* transcript levels were significantly reduced in SVZ cells from *Nestin-CreER*^{T2}; *Prdm16*$^{fl/fl}$ mice by qRT–PCR (Fig. 6B). Although hydrocephalus was evident in 1-mo-old *Nestin-Cre; Prdm16*$^{fl/fl}$ mice, as indicated by enlarged lateral ventricles (Fig. 6C), we did not detect any sign of hydrocephalus in 1-mo-old *Nestin-CreER*^{T2}; *Prdm16*$^{fl/fl}$ mice (Fig. 6D,E). Compared with control littermates, *Nestin-*

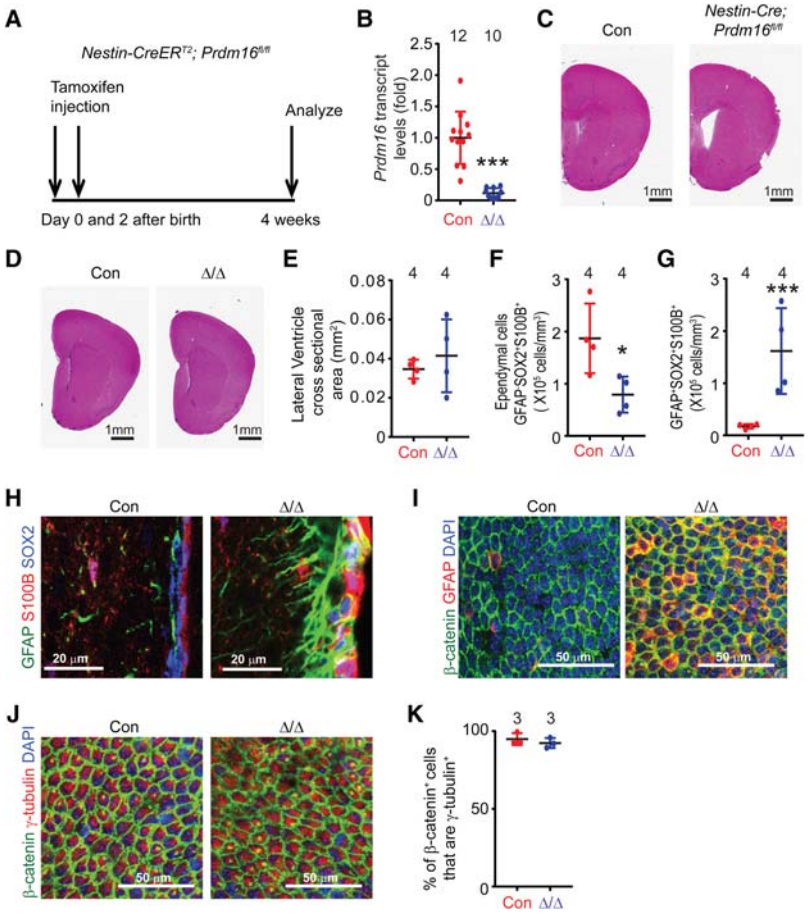

Figure 6. Prdm16 is required postnatally for the normal differentiation of ependymal cells. *Nestin-CreER^{T2}; Prdm16$^{fl/fl}$* mice (Δ/Δ) and littermate controls (Con) were treated with tamoxifen at P0 and P2 and then analyzed 1 mo later. All data represent mean ± SD. (*A*) A schematic of the experiment. (*B*) *Prdm16* transcript levels in the SVZ by qRT–PCR 1 mo after tamoxifen treatment. (*C*) For comparison purposes, representative images of hematoxylin and eosin-stained coronal sections from *Nestin-Cre; Prdm16$^{fl/fl}$* and littermate control mice at 1 mo of age. (*D*) Representative images of hematoxylin and eosin-stained coronal sections 1 mo after tamoxifen treatment of *Nestin-CreER^{T2}; Prdm16$^{fl/fl}$* and littermate control mice. (*E*) Lateral ventricle cross-sectional area (four to five sections per mouse, cut 300 μm apart, beginning at the rostral end of the lateral ventricle) of *Nestin-CreER^{T2}; Prdm16$^{fl/fl}$* and littermate control mice. (*F*) The number of GFAP$^-$Sox2$^+$S100B$^+$ ependymal cells was decreased in the SVZ of *Nestin-CreER^{T2}; Prdm16$^{fl/fl}$* mice compared with littermate controls. (*G*) GFAP$^+$S100B$^+$Sox2$^+$ cells with long processes were common in the SVZ of *Nestin-CreER^{T2}; Prdm16$^{fl/fl}$* mice but not littermate controls. (*H*) Representative images of SVZ sections showing the increased numbers of GFAP$^+$S100B$^+$Sox2$^+$ cells with long processes on the ventricular surface of *Nestin-CreER^{T2}; Prdm16$^{fl/fl}$* mice. (*I*) En face images of the lateral wall of the lateral ventricle surface showing that β-catenin$^+$ ependymal cells showed unusual GFAP expression in *Nestin-CreER^{T2}; Prdm16$^{fl/fl}$* mice. (*J*,*K*) Nearly all β-catenin$^+$ cells on the lateral ventricle surface were also γ-tubulin$^+$ in mice of both genotypes. The statistical significance of differences between genotypes was assessed by Mann-Whitney (*K*) or Student's *t*-tests (*B*, *E–G*). (*) $P < 0.05$; (***) $P < 0.001$. The numbers of replicates in each treatment are shown at the *top* of each graph.

CreER^{T2}; Prdm16$^{fl/fl}$ mice had a significantly reduced number of GFAP$^-$Sox2$^+$S100B$^+$ ependymal cells (Fig. 6F, H) and a significantly increased number of GFAP$^+$ Sox2$^+$S100B$^+$ cells lining the lateral ventricle (Fig. 6G). Although ependymal cells do not usually express GFAP, the GFAP$^+$Sox2$^+$S100B$^+$ cells observed in *Nestin-CreER^{T2}; Prdm16$^{fl/fl}$* mice (Fig. 6I) were ciliated (Fig. 6J,K). These data suggest that postnatal deletion of *Prdm16* from Nestin-expressing stem/progenitor cells led to abnormally differentiated ependymal cells that retained GFAP expression. Nonetheless, these cells retained adequate ependymal cell function to avoid the development of hydrocephalus. Taken together, our data indicate that Prdm16 acts primarily during fetal development to promote the formation of ependymal cells, but there is an ongoing requirement for Prdm16 postnatally for normal differentiation.

Prdm16 is required for the expression of Foxj1

Radial glial cells proliferate during embryogenesis and differentiate into ciliated ependymal cells by the second postnatal week (Spassky et al. 2005). Using *Prdm16$^{LacZ/+}$* mice, we confirmed that Prdm16 was expressed by most Nestin$^+$ neural stem cells in the SVZ at P4 (Fig. 7A). *Prdm16* was efficiently deleted from the SVZ of *Nestin-Cre; Prdm16$^{fl/fl}$* mice by P4 (Fig. 7B). At this stage, the number of Sox2-positive neural stem/progenitor cells did not significantly differ between *Nestin-Cre; Prdm16$^{fl/fl}$* mice and littermate controls (Fig. 7C).

To assess the mechanism by which Prdm16 regulates the formation of ependymal cells, we performed RNA sequencing (RNA-seq) analysis on P4 SVZ cells from *Nestin-Cre; Prdm16$^{fl/fl}$* mice and littermate controls ($n = 3$ independent samples per genotype, each from different mice). We identified 130 gene products that were significantly differentially expressed between *Prdm16*-deficient and control SVZ cells (fold change >2.5; false discovery rate [FDR] $q < 0.005$; fragments per kilobase per million mapped fragments [FPKM] > 1 in all of the samples from at least one of the cell populations). Of these, 103 were expressed at significantly lower levels in *Prdm16*-deficient cells (Supplemental Table S1), and 27 were significantly more highly expressed (Supplemental Table S2). Strikingly, 20 of these gene products (19%) were cilia components, all of which were expressed at significantly lower levels in *Prdm16*-deficient cells. These included Foxj1 and Myb (transcription factors that promote ependymal cell

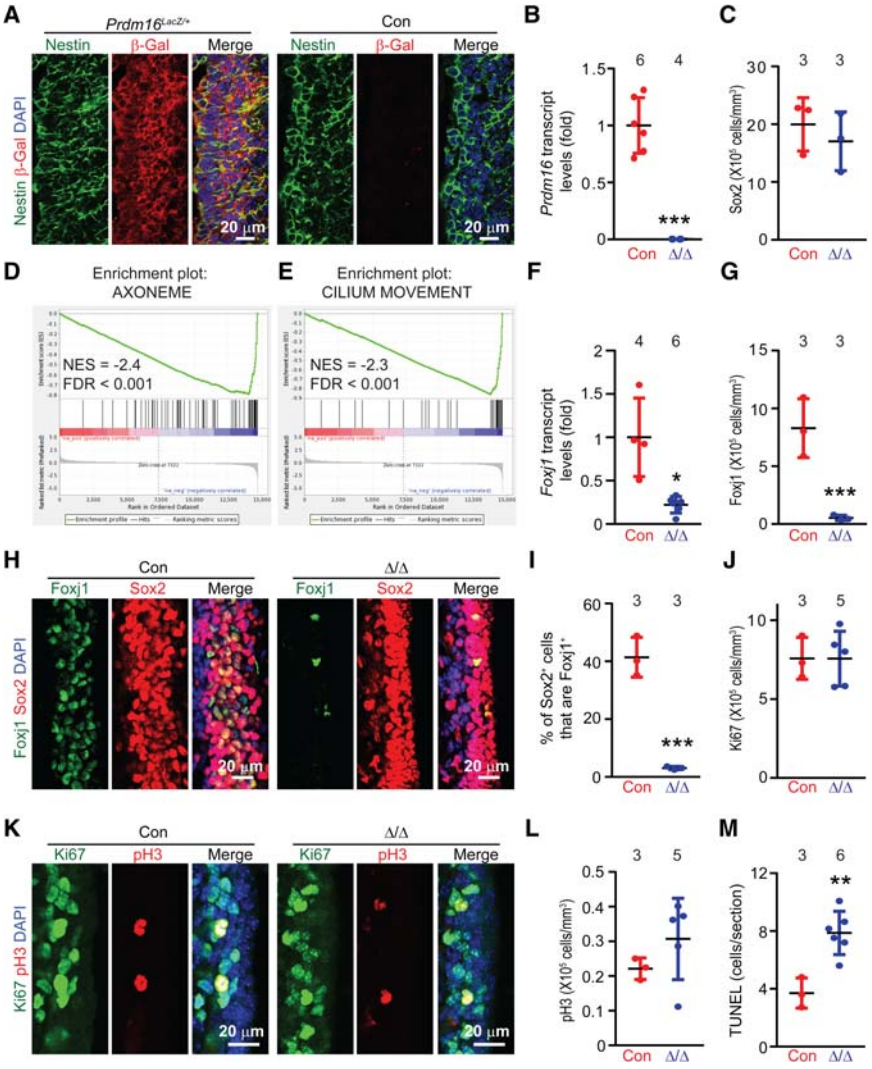

Figure 7. Prdm16 is required for the expression of Foxj1 in neural stem/progenitor cells at P4, when ependymal cells are normally differentiating. All of the analyses were performed on *Nestin-Cre; Prdm16*$^{fl/fl}$ (Δ/Δ), *Prdm16*$^{LacZ/+}$, or littermate control (Con) mice at P4. All data represent mean ± SD from two or three independent experiments. (*A*) In *Prdm16*$^{LacZ/+}$ mice, β-gal colocalized with Nestin in the SVZ at P4. (*B*) qRT–PCR analysis of *Prdm16* transcript levels in the SVZ. (*C*) The number of Sox2$^+$ neural stem/progenitor cells per cubic millimeter in the SVZ. (*D*,*E*) Gene set enrichment analysis showing "axoneme" and "cilium movement" gene sets that were significantly depleted in *Nestin-Cre; Prdm16*$^{fl/fl}$ mice. (NES) Normalized enrichment score; (FDR) false discovery rate. (*F*) qRT–PCR analysis of *Foxj1* transcript levels in the SVZ. (*G–I*) The number of Foxj1$^+$ cells per cubic millimeter in the SVZ (*G*); representative images of Foxj1, Sox2, and DAPI staining in the SVZ (*H*); and the percentage of Sox2$^+$ cells that were Foxj1$^+$ in the SVZ (*I*). (*J–M*) The number of Ki67$^+$ proliferating cells per cubic millimeter in the SVZ (*J*); representative images of Ki67, phospho-Histone 3 (pH3), and DAPI staining in the SVZ (*K*); the number of pH3$^+$ proliferating cells per cubic millimeter in the SVZ (*L*); and the number TUNEL$^+$ dying cells per SVZ section (*M*). The statistical significance of differences between genotypes was assessed using Welch's test (*F*) and Student's *t*-tests (*B*,*C*,*G*,*I*,*J*,*L*,*M*). (*) $P < 0.05$; (**) $P < 0.01$; (***) $P < 0.001$. The numbers of replicates in each treatment are shown at the *top* of each graph.

differentiation) (Malaterre et al. 2008; Yu et al. 2008; Jacquet et al. 2009; Tan et al. 2013) as well as 18 ciliary structural proteins (Ak7, Spata18, Ccdc113, Dynlrb2, Cfap126, Rsph1, Tekt4, Spag16, Efhc1, Ccno, Ccdc135, Ccdc170, Rsph4a, Ak8, Dnajb13, Spef2, Spa17, and Fam161a). Based on an analysis of cilium-related gene sets, we estimated that there are ~400 genes that encode products required for the formation or function of cilia in the genome (~1.7% of the genome). This indicates that cilium-related genes were highly enriched among genes that were down-regulated in *Prdm16*-deficient SVZ cells ($P < 0.0001$ by binomial test).

Gene set enrichment analysis revealed six gene sets that were significantly enriched (FDR $q < 0.001$) among genes that were down-regulated (normalized enrichment score [NES] ≤−2.3) in *Prdm16*-deficient cells (Supplemental Table S3). Five of the six gene sets were cilium-related, including "ciliary cytoplasm," "axoneme," "axoneme assembly," "cilium movement," and "motile cilium" (Fig. 7D,E). We found nine gene sets that were significantly enriched (FDR $q < 0.001$) among genes that were up-regulated (NES ≥2,3) in *Prdm16*-deficient cells (Supplemental Table S4). None were related to cilia. Most were gene sets related to neuronal differentiation.

Foxj1 is required for the differentiation of radial glia into ependymal cells (Yu et al. 2008; Jacquet et al. 2009). Therefore, the reduced expression of *Foxj1* in the absence of Prdm16 offers a potential mechanism to explain the reduced generation of ependymal cells in *Nestin-Cre; Prdm16*$^{fl/fl}$ mice. To confirm the reduced Foxj1 expression, we performed qRT–PCR on SVZ cells from P4 *Nestin-Cre; Prdm16*$^{fl/fl}$ and littermate control mice. We found that *Foxj1* transcript levels were 4.5-fold ± 1.9-fold lower in *Nestin-Cre; Prdm16*$^{fl/fl}$ SVZ cells as compared with control SVZ cells (Fig. 7F). We also performed immunofluorescence analysis for Foxj1 in sections through the P4 SVZ. In control SVZ, there were $8.3 \times 10^5 \pm 2.5 \times 10^5$ Foxj1$^+$ cells per cubic millimeter, while in the *Nestin-Cre; Prdm16*$^{fl/fl}$ SVZ, there were only $0.53 \times 10^5 \pm 0.23 \times 10^5$ Foxj1$^+$ cells per cubic millimeter (a 94% reduction) (Fig. 7G). Furthermore, 41% ± 6.9% of Sox2$^+$ cells were Foxj1$^+$ in the control SVZ, and only 3.1% ± 0.6% of Sox2$^+$ cells were Foxj1$^+$ in *Nestin-Cre; Prdm16*$^{fl/fl}$ SVZ (a 92% reduction) (Fig. 7H,I). Prdm16 is thus required

for Foxj1 expression by neural stem/progenitor cells in the SVZ.

To investigate whether Prdm16 directly regulates *Foxj1*, we performed ChIP-seq (chromatin immunoprecipitation [ChIP] combined with high-throughput sequencing) analysis using a Prdm16 polyclonal antibody in P4 SVZ samples. However, we did not find convincing Prdm16-binding sites associated with *Foxj1* or other cilia-related genes whose expression declined in the absence of Prdm16 (data not shown). Indeed, we observed very few convincing Prdm16-binding sites genome-wide. There is increasing evidence that Prdm16 regulates the expression of some genes by binding to protein complexes that are difficult to detect by ChIP-seq rather than by direct binding to DNA (Harms et al. 2015; Iida et al. 2015; Ishibashi and Seale 2015). Therefore, it remains unclear whether Prdm16 directly or indirectly regulates the expression of *Foxj1* and other genes required for ciliogenesis.

We did not observe any difference in the numbers of $Ki67^+$ or $pH3^+$ proliferating cells *in Nestin-Cre; $Prdm16^{fl/fl}$* mice as compared with littermate control mice at P4 (Fig. 7J–L) but did observe significantly increased apoptosis in the SVZ of *Nestin-Cre; $Prdm16^{fl/fl}$* mice as compared with control mice at P4 (Fig. 7M). These data suggest that in the absence of Prdm16, at least some neural stem/progenitor cells in the postnatal SVZ undergo cell death. Given the accumulation of an unusual population of $GFAP^+Sox2^+S100B^+$ cells with radial processes at the ventricular surface of *Nestin-Cre; $Prdm16^{fl/fl}$*, but not control, mice (Fig. 5A,B), some of the $Sox2^+$ cells that would normally differentiate to ependymal cells may acquire an abnormal glial identity.

Discussion

1p36 microdeletion syndrome, which affects a genomic locus that includes *Prdm16* as well as other genes, is associated with severe mental retardation, seizures, distinctive facial features, hydrocephalus, and heart abnormalities. Although there is evidence that loss of *Prdm16* contributes to the craniofacial and cardiac defects in this syndrome (Bjork et al. 2010; Arndt et al. 2013), the cause of hydrocephalus in 1p36 microdeletion syndrome is not understood. Our study indicates that, in addition to being required for fetal and adult neural stem cell function, Prdm16 is required for the differentiation of neural stem cells into ciliated ependymal cells (Fig. 7). Prdm16 was required in neural stem/progenitors for the expression of Foxj1, a transcription factor necessary for ependymal cell differentiation (Yu et al. 2008; Jacquet et al. 2009). The hydrocephalus that we observed after deletion of *Prdm16* using *Nestin*-Cre is consistent with the hydrocephalus observed after deletion of *Foxj1* (Jacquet et al. 2009).

Using ChIP-seq analysis, we were unable to detect convincing localization of Prdm16 to the *Foxj1* promoter or to other loci that encode genes involved in ciliogenesis. However, Prdm16 appears to often regulate the expression of genes by binding to, and regulating the function of, other transcription factors (Nishikata et al. 2003; Harms et al. 2015; Iida et al. 2015). Therefore, it remains unclear whether Prdm16 directly or indirectly regulates the expression of genes involved in ciliogenesis.

Although some ciliated cells remained in *Nestin-Cre; $Prdm16^{fl/fl}$* mice, the cilia movement was abnormal and caused abnormal CSF flow (Fig. 5). Although a loss of motile cilia is known to cause hydrocephalus in mice (Jacquet et al. 2009; Del Bigio 2010; Tissir et al. 2010; Ohata et al. 2014), magnetic resonance imaging (MRI) scanning studies show that CSF overproduction, CSF absorption defects, and aqueduct stenosis can also lead to hydrocephalus in humans (Kahle et al. 2016). Due to the small size of the mouse brain, it is technically challenging to test these possibilities in mice by MRI. Therefore, the simplest interpretation of our data is that the hydrocephalus observed in *Nestin-Cre; $Prdm16^{fl/fl}$* mice is caused by a failure of ependymal cell function and abnormal CSF flow, although it is possible that other congenital defects in the brain contribute to this phenotype.

In contrast to the defects in ependymal cell differentiation and hydrocephalus in *Nestin-Cre; $Prdm16^{fl/fl}$* mice, conditional deletion of *Prdm16* during adulthood in *Nestin-$CreER^{T2}$; $Prdm16^{fl/fl}$* mice did not lead to defects in ependymal cell differentiation, cilia function, or hydrocephalus (Supplemental Fig. S3). Nonetheless, these mice continued to exhibit SVZ neural stem cell depletion, little ability to form multipotent or self-renewing neurospheres in culture (Fig. 3), and reduced SVZ proliferation and neurogenesis (Fig. 4). Thus, these defects in neural stem cell function are not secondary consequences of hydrocephalus, as they were observed even in *Nestin-$CreER^{T2}$; $Prdm16^{fl/fl}$* mice that never developed hydrocephalus. Thus, Prdm16 independently appears to regulate multiple aspects of neural stem cell function, including neural stem cell maintenance, neurogenesis, and ependymal cell differentiation.

Materials and methods

Mice

All mice were housed at the Animal Resource Center of the University of Texas Southwestern Medical Center. All protocols were approved by the University of Texas Southwestern Institutional Animal Care and Use Committee. Mice were housed in standard cages that contained three to five mice per cage, with water and standard diet ad libitum and a 12-h light/dark cycle. Both male and female mice were analyzed in all experiments. *Nestin-Cre* mice were obtained from Jackson Laboratory (Tronche et al. 1999). *Nestin-$CreER^{T2}$* mice were provided by G. Fishell (Balordi and Fishell 2007). *$Prdm16^{fl/fl}$* mice were provided by B. Spiegelman (Cohen et al. 2014). *$Prdm16^{Gt(OST67423)Lex}$* mice were obtained from the National Institutes of Health Mutant Mouse Regional Resource Center (http://www.mmrrc.org). All mice were backcrossed onto a C57BL/Ka background for at least three generations prior to analysis. Control mice were a combination of *$Prdm16^{fl/fl}$*, *$Prdm16^{fl/+}$*, and *$Prdm16^{+/+}$* mice. We did not observe any phenotypic differences among mice with these genotypes. For tamoxifen treatment, tamoxifen (Sigma, T5648) was dissolved in 90% corn oil/10% ethanol at 20 mg/mL and injected at 100 mg/kg per day intraperitoneally for three consecutive days,

and tamoxifen citrate (Sigma or Spectrum Chemical) was given in the chow for 1 mo at 400 mg/kg with 5% sucrose (Harlan) starting at 2 mo of age. Mice were fed a standard diet for at least 2 wk before analysis. For tamoxifen treatment of postnatal mice, tamoxifen was dissolved in 90% corn oil/10% ethanol at 2.5 mg/mL, and 20 µL was injected into the stomachs of P0 and P2 mice. Mice were analyzed 1 mo after tamoxifen treatment.

SVZ cell preparation

SVZs from adult (2- to 10-mo-old) mice were dissected and dissociated as described (Mich et al. 2014). Briefly, SVZs were minced and digested with 700 µL of trypsin solution (Ca and Mg-free Hank's buffered salt solution [HBSS], 10 mM HEPES, 0.5 mM EDTA, 0.25 mg/mL trypsin [EMD Millipore], 10 µg/mL DNase I [Roche] at pH 7.6) for 15 min at 37°C. Digestion was quenched with 2 vol of staining medium (440 mL of Leibovitz L-15 medium, 50 mL of water, 5 mL of 1 M HEPES at pH 7.3–7.4, 5 mL of 100× penicillin–streptomycin [Pen-Strep], 1 g of bovine serum albumin [Sigma, A7030]) and 100 µg/mL trypsin inhibitor (Sigma, T6522). Digested cells were centrifuged at 491*g* for 8 min at 4°C, fresh staining medium was added, and the pieces were triturated in 700 µL by gently drawing them into a P1000 pipetman and expelling them 20 times without forming bubbles. The cell suspension was then filtered through a 45-µm mesh, counted on a hemocytometer, and added to culture or processed for flow cytometry. Neurosphere formation, self-renewal, and differentiation assays were performed as described previously (Mich et al. 2014).

For additional methodological details concerning PCR genotyping of mice, immunohistochemistry, flow cytometry, microbead flow analysis, scanning electron microscopy, hematoxylin and eosin staining, analysis of RNA-seq data, cell quantification, and statistics, see the Supplemental Material.

Accession numbers

RNA-seq data have been deposited in the Sequence Read Archive public database with accession number PRJNA339165 and submission number SUB1780202.

Acknowledgments

We thank Dr. Bruce Spiegelman for providing *Prdm16*^{flox} mice, and Dr. Patrick Seale for providing anti-Prdm16 antibody and technical advice for using it for ChIP. We also thank Vishal Khivansara, Saikat Mukhopadhyay, Jian Xu, Andrew DeVilbiss, and Woo-Ping Ge for discussing results. We thank BioHPC at University of Texas Southwestern for providing high-performance computing resources, and the Live Cell Imaging Facility (National Institute of Health [NIH] S10RR029731), the Electron Microscopy Core (NIH S10OD020103), the Molecular Pathology Core, and the Quantitative Morphology Core at University of Texas Southwestern Medical Center. S.J.M. is a Howard Hughes Medical Institute Investigator, the Mary McDermott Cook Chair in Pediatric Genetics, the Kathryne and Gene Bishop Distinguished Chair in Pediatric Research, the director of the Hamon Laboratory for Stem Cells and Cancer, and a Cancer Prevention and Research Institute of Texas Scholar. This work was supported by the NIH (R37 AG024945 and R01 NS040750). I.S.S. was supported by a post-doctoral fellowship from the American Heart Association. I.S.S. performed most of the experiments. M.A. and R.J.B. performed some of the experiments in Figures 2, 3, and 6. Z.Z. analyzed the RNA-seq data and performed the statistical analyses. I.S.S. and S.J.M. designed the experiments, interpreted the results, and wrote the manuscript.

References

Aguilo F, Avagyan S, Labar A, Sevilla A, Lee DF, Kumar P, Lemischka IR, Zhou BY, Snoeck HW. 2011. Prdm16 is a physiologic regulator of hematopoietic stem cells. *Blood* **117:** 5057–5066.

Aimone JB, Li Y, Lee SW, Clemenson GD, Deng W, Gage FH. 2014. Regulation and function of adult neurogenesis: from genes to cognition. *Physiol Rev* **94:** 991–1026.

Alvarez-Buylla A, Kohwi M, Nguyen TM, Merkle FT. 2008. The heterogeneity of adult neural stem cells and the emerging complexity of their niche. *Cold Spring Harb Symp Quant Biol* **73:** 357–365.

Arndt AK, Schafer S, Drenckhahn JD, Sabeh MK, Plovie ER, Caliebe A, Klopocki E, Musso G, Werdich AA, Kalwa H, et al. 2013. Fine mapping of the 1p36 deletion syndrome identifies mutation of PRDM16 as a cause of cardiomyopathy. *Am J Hum Genet* **93:** 67–77.

Balordi F, Fishell G. 2007. Mosaic removal of hedgehog signaling in the adult SVZ reveals that the residual wild-type stem cells have a limited capacity for self-renewal. *J Neurosci* **27:** 14248–14259.

Battaglia A, Hoyme HE, Dallapiccola B, Zackai E, Hudgins L, McDonald-McGinn D, Bahi-Buisson N, Romano C, Williams CA, Brailey LL, et al. 2008. Further delineation of deletion 1p36 syndrome in 60 patients: a recognizable phenotype and common cause of developmental delay and mental retardation. *Pediatrics* **121:** 404–410.

Bjork BC, Turbe-Doan A, Prysak M, Herron BJ, Beier DR. 2010. Prdm16 is required for normal palatogenesis in mice. *Hum Mol Genet* **19:** 774–789.

Brazel CY, Limke TL, Osborne JK, Miura T, Cai J, Pevny L, Rao MS. 2005. Sox2 expression defines a heterogeneous population of neurosphere-forming cells in the adult murine brain. *Aging cell* **4:** 197–207.

Chuikov S, Levi BP, Smith ML, Morrison SJ. 2010. Prdm16 promotes stem cell maintenance in multiple tissues, partly by regulating oxidative stress. *Nat Cell Biol* **12:** 999–1006.

Codega P, Silva-Vargas V, Paul A, Maldonado-Soto AR, Deleo AM, Pastrana E, Doetsch F. 2014. Prospective identification and purification of quiescent adult neural stem cells from their in vivo niche. *Neuron* **82:** 545–559.

Cohen P, Levy JD, Zhang Y, Frontini A, Kolodin DP, Svensson KJ, Lo JC, Zeng X, Ye L, Khandekar MJ, et al. 2014. Ablation of PRDM16 and beige adipose causes metabolic dysfunction and a subcutaneous to visceral fat switch. *Cell* **156:** 304–316.

Del Bigio MR. 2010. Ependymal cells: biology and pathology. *Acta Neuropathol* **119:** 55–73.

Doetsch F, Caille I, Lim DA, Garcia-Verdugo JM, Alvarez-Buylla A. 1999. Subventricular zone astrocytes are neural stem cells in the adult mammalian brain. *Cell* **97:** 703–716.

Faubel R, Westendorf C, Bodenschatz E, Eichele G. 2016. Cilia-based flow network in the brain ventricles. *Science* **353:** 176–178.

Ferri AL, Cavallaro M, Braida D, Di Cristofano A, Canta A, Vezzani A, Ottolenghi S, Pandolfi PP, Sala M, DeBiasi S, et al. 2004. Sox2 deficiency causes neurodegeneration and impaired neurogenesis in the adult mouse brain. *Development* **131:** 3805–3819.

Fliegauf M, Benzing T, Omran H. 2007. When cilia go bad: cilia defects and ciliopathies. *Nat Rev Mol Cell Biol* **8:** 880–893.

Gleeson JG, Lin PT, Flanagan LA, Walsh CA. 1999. Doublecortin is a microtubule-associated protein and is expressed widely by migrating neurons. *Neuron* **23:** 257–271.

Gonzalez-Cano L, Fuertes-Alvarez S, Robledinos-Anton N, Bizy A, Villena-Cortes A, Farinas I, Marques MM, Marin MC. 2016. p73 is required for ependymal cell maturation and neurogenic SVZ cytoarchitecture. *Dev Neurobiol* **76:** 730–747.

Harms MJ, Lim HW, Ho Y, Shapira SN, Ishibashi J, Rajakumari S, Steger DJ, Lazar MA, Won KJ, Seale P. 2015. PRDM16 binds MED1 and controls chromatin architecture to determine a brown fat transcriptional program. *Genes Dev* **29:** 298–307.

Hohenauer T, Moore AW. 2012. The Prdm family: expanding roles in stem cells and development. *Development* **139:** 2267–2282.

Iida S, Chen W, Nakadai T, Ohkuma Y, Roeder RG. 2015. PRDM16 enhances nuclear receptor-dependent transcription of the brown fat-specific Ucp1 gene through interactions with Mediator subunit MED1. *Genes Dev* **29:** 308–321.

Ishibashi J, Seale P. 2015. Functions of Prdm16 in thermogenic fat cells. *Temperature* **2:** 65–72.

Jacquet BV, Salinas-Mondragon R, Liang H, Therit B, Buie JD, Dykstra M, Campbell K, Ostrowski LE, Brody SL, Ghashghaei HT. 2009. FoxJ1-dependent gene expression is required for differentiation of radial glia into ependymal cells and a subset of astrocytes in the postnatal brain. *Development* **136:** 4021–4031.

Kahle KT, Kulkarni AV, Limbrick DD Jr, Warf BC. 2016. Hydrocephalus in children. *Lancet* **387:** 788–799.

Kuo CT, Mirzadeh Z, Soriano-Navarro M, Rasin M, Wang D, Shen J, Sestan N, Garcia-Verdugo J, Alvarez-Buylla A, Jan LY, et al. 2006. Postnatal deletion of Numb/Numblike reveals repair and remodeling capacity in the subventricular neurogenic niche. *Cell* **127:** 1253–1264.

Kyrousi C, Arbi M, Pilz GA, Pefani DE, Lalioti ME, Ninkovic J, Gotz M, Lygerou Z, Taraviras S. 2015. Mcidas and GemC1 are key regulators for the generation of multiciliated ependymal cells in the adult neurogenic niche. *Development* **142:** 3661–3674.

Lim DA, Alvarez-Buylla A. 2014. Adult neural stem cells stake their ground. *Trends Neurosci* **37:** 563–571.

Lim DA, Tramontin AD, Trevejo JM, Herrera DG, Garcia-Verdugo JM, Alvarez-Buylla A. 2000. Noggin antagonizes BMP signaling to create a niche for adult neurogenesis. *Neuron* **28:** 713–726.

Liu M, Guan Z. 2016. Ulk4 is essential for ciliogenesis and CSF flow. *J Neurosci* **36:** 7589–7600.

Luchsinger LL, de Almeida MJ, Corrigan DJ, Mumau M, Snoeck HW. 2016. Mitofusin 2 maintains haematopoietic stem cells with extensive lymphoid potential. *Nature* **529:** 528–531.

Lui JH, Hansen DV, Kriegstein AR. 2011. Development and evolution of the human neocortex. *Cell* **146:** 18–36.

Malaterre J, Mantamadiotis T, Dworkin S, Lightowler S, Yang Q, Ransome MI, Turnley AM, Nichols NR, Emambokus NR, Frampton J, et al. 2008. c-Myb is required for neural progenitor cell proliferation and maintenance of the neural stem cell niche in adult brain. *Stem Cells* **26:** 173–181.

Mich JK, Signer RA, Nakada D, Pineda A, Burgess RJ, Vue TY, Johnson JE, Morrison SJ. 2014. Prospective identification of functionally distinct stem cells and neurosphere-initiating cells in adult mouse forebrain. *eLife* **3:** e02669.

Mirzadeh Z, Merkle FT, Soriano-Navarro M, Garcia-Verdugo JM, Alvarez-Buylla A. 2008. Neural stem cells confer unique pinwheel architecture to the ventricular surface in neurogenic regions of the adult brain. *Cell Stem Cell* **3:** 265–278.

Mirzadeh Z, Doetsch F, Sawamoto K, Wichterle H, Alvarez-Buylla A. 2010a. The subventricular zone en-face: wholemount staining and ependymal flow. *J Vis Exp* doi: 10.3791/1938.

Mirzadeh Z, Han YG, Soriano-Navarro M, Garcia-Verdugo JM, Alvarez-Buylla A. 2010b. Cilia organize ependymal planar polarity. *J Neurosci* **30:** 2600–2610.

Mochizuki N, Shimizu S, Nagasawa T, Tanaka H, Taniwaki M, Yokota J, Morishita K. 2000. A novel gene, MEL1, mapped to 1p36.3 is highly homologous to the MDS1/EVI1 gene and is transcriptionally activated in t(1;3)(p36;q21)-positive leukemia cells. *Blood* **96:** 3209–3214.

Nishikata I, Sasaki H, Iga M, Tateno Y, Imayoshi S, Asou N, Nakamura T, Morishita K. 2003. A novel EVI1 gene family, MEL1, lacking a PR domain (MEL1S) is expressed mainly in t(1;3)(p36;q21)-positive AML and blocks G-CSF-induced myeloid differentiation. *Blood* **102:** 3323–3332.

Ohata S, Nakatani J, Herranz-Perez V, Cheng J, Belinson H, Inubushi T, Snider WD, Garcia-Verdugo JM, Wynshaw-Boris A, Alvarez-Buylla A. 2014. Loss of Dishevelleds disrupts planar polarity in ependymal motile cilia and results in hydrocephalus. *Neuron* **83:** 558–571.

Park R, Moon UY, Park JY, Hughes LJ, Johnson RL, Cho SH, Kim S. 2016. Yap is required for ependymal integrity and is suppressed in LPA-induced hydrocephalus. *Nat Commun* **7:** 10329.

Porlan E, Marti-Prado B, Morante-Redolat JM, Consiglio A, Delgado AC, Kypta R, Lopez-Otin C, Kirstein M, Farinas I. 2014. MT5-MMP regulates adult neural stem cell functional quiescence through the cleavage of N-cadherin. *Nat Cell Biol* **16:** 629–638.

Sawamoto K, Wichterle H, Gonzalez-Perez O, Cholfin JA, Yamada M, Spassky N, Murcia NS, Garcia-Verdugo JM, Marin O, Rubenstein JL, et al. 2006. New neurons follow the flow of cerebrospinal fluid in the adult brain. *Science* **311:** 629–632.

Seale P, Bjork B, Yang W, Kajimura S, Chin S, Kuang S, Scime A, Devarakonda S, Conroe HM, Erdjument-Bromage H, et al. 2008. PRDM16 controls a brown fat/skeletal muscle switch. *Nature* **454:** 961–967.

Shing DC, Trubia M, Marchesi F, Radaelli E, Belloni E, Tapinassi C, Scanziani E, Mecucci C, Crescenzi B, Lahortiga I, et al. 2007. Overexpression of sPRDM16 coupled with loss of p53 induces myeloid leukemias in mice. *J Clin Invest* **117:** 3696–3707.

Spassky N, Merkle FT, Flames N, Tramontin AD, Garcia-Verdugo JM, Alvarez-Buylla A. 2005. Adult ependymal cells are postmitotic and are derived from radial glial cells during embryogenesis. *J Neurosci* **25:** 10–18.

Stubbs JL, Vladar EK, Axelrod JD, Kintner C. 2012. Multicilin promotes centriole assembly and ciliogenesis during multiciliate cell differentiation. *Nat Cell Biol* **14:** 140–147.

Tan FE, Vladar EK, Ma L, Fuentealba LC, Hoh R, Espinoza FH, Axelrod JD, Alvarez-Buylla A, Stearns T, Kintner C, et al. 2013. Myb promotes centriole amplification and later steps of the multiciliogenesis program. *Development* **140:** 4277–4286.

Tissir F, Qu Y, Montcouquiol M, Zhou L, Komatsu K, Shi D, Fujimori T, Labeau J, Tyteca D, Courtoy P, et al. 2010. Lack of cadherins Celsr2 and Celsr3 impairs ependymal ciliogenesis, leading to fatal hydrocephalus. *Nat Neurosci* **13:** 700–707.

Tramontin AD, Garcia-Verdugo JM, Lim DA, Alvarez-Buylla A. 2003. Postnatal development of radial glia and the ventricular zone (VZ): a continuum of the neural stem cell compartment. *Cereb Cortex* **13:** 580–587.

Tronche F, Kellendonk C, Kretz O, Gass P, Anlag K, Orban PC, Bock R, Klein R, Schutz G. 1999. Disruption of the glucocorticoid receptor gene in the nervous system results in reduced anxiety. *Nat Genet* **23:** 99–103.

Tully HM, Dobyns WB. 2014. Infantile hydrocephalus: a review of epidemiology, classification and causes. *Eur J Med Genet* **57:** 359–368.

Wang H, Kane AW, Lee C, Ahn S. 2014. Gli3 repressor controls cell fates and cell adhesion for proper establishment of neurogenic niche. *Cell Rep* **8:** 1093–1104.

Yang A, Walker N, Bronson R, Kaghad M, Oosterwegel M, Bonnin J, Vagner C, Bonnet H, Dikkes P, Sharpe A, et al. 2000. p73-deficient mice have neurological, pheromonal and inflammatory defects but lack spontaneous tumours. *Nature* **404:** 99–103.

Yu X, Ng CP, Habacher H, Roy S. 2008. Foxj1 transcription factors are master regulators of the motile ciliogenic program. *Nat Genet* **40:** 1445–1453.